

CHAPTER 91

Local Movements of Sand in the Surf Zone

Kazumasa KATOH¹ and Norio TANAKA²

Abstract

The fluorescent sand tracers are injected in a point in the surf zone. Core samples are taken from the sixteen points on the circumference with the time intervals of fifteen minutes for about five hours. At the same time, the horizontal two components of fluid velocities are measured at the injection point by using an electromagnetic currentmeter. The field observations have been carried out three times on two beaches facing to the Pacific Ocean. The relations between the local sand movements and the fluid dynamics are examined on the basis of the data obtained.

1. Introduction

The study on the local sand transport in the surf zone is regarded as one of the very important themes in the coastal engineering, and it is earnestly hoped to make clear the actual conditions of sediment dynamics in the surf zone. There is, however, a major obstacle to further understanding of the local sand transport, or nearshore sediment dynamics, that is to say, the lack of instruments which can directly measure the sediment transport.

Nadaoka, Tanaka and Katoh (1981) developed the technique to use the fluorescent sand tracer for measuring the local sand movements in the surf zone, and examined its capability by applying it to the field, Ajigaura Beach in Japan. The result proved the technique quite promising, and we decided to explore its possibility further. The field observations with the fluorescent sand tracer have been carried on two beaches facing to the Pacific Ocean - Oarai Beach in 1981 and Sudahama Beach in 1982 and 1983, in Japan.

In this report, based on the data obtained by this method on these beaches, we examine the local sand movements such as the advection speed of sand tracer, the mixing depth into the sea bottom, the local sand transport rate, and so on.

1) Chief of Littoral Drift Laboratory, Hydraulic Engineering Division, Port and Harbour Research Institute, 1-1, 3-chome, Nagase, Yokosuka, Japan. 2) Nippon Tetrapod Co., LTD., Japan (Former Director of Marine Hydrodynamics Division, PHRI)

2. Field Observations

2.1 Observation procedure

An outline of the observation procedure employed in the field using fluorescent sand tracer is as follows. First of all, a circle with the radius of 8.75 meters is established in the surf zone at an observation site. In practice, one pipe is set at the center of circle and sixteen pipes are set at the points which divide the circumference into sixteen arcs. An electromagnetic currentmeter is also set near the center of circle to measure the two horizontal components of the current velocity.

Three different colors of the fluorescent sand tracers, red, blue and yellow-green, are prepared in advance by utilizing the sand which have been previously removed from the beach face at the observation site. The observation starts at the time when one of the three colors of the tracers is injected at the center of circle. The remaining two colors of tracers are injected at the center at the time of one and two hours after the first injection, respectively. The volume of each sand tracer injected is 5 kilograms at a time. A sampling of the sand tracer at the sixteen points on the circumference is started 5 minutes after the first injection and is repeated with the time interval of 15 minutes, being 21 times for the typical case.

Core samples are taken at all the sixteen points as shown in Fig.1. The sampling procedure done by frogmen is as follows. (a) A transparent acrylic pipe of about 130 centimeters in length, 3.4 centimeters in inner diameter and 3 millimeters in thickness is brought to the sampling point by a frogman. (b) The acrylic pipe is pushed into the sea bottom by 20 to 30 centimeters. (c) The upper end of pipe is sealed with a rubber stopper. (d) The pipe is pulled out with the core sample inside it. (e) Immediately after it, the lower end of pipe is sealed with another rubber stopper, and the pipe is brought to the shore.

After removing the sea water, the core sample is slowly pushed out from the pipe onto a flat plate by using a piston. In almost all cases, the core sample was able to be taken out in a cylindrical shape without

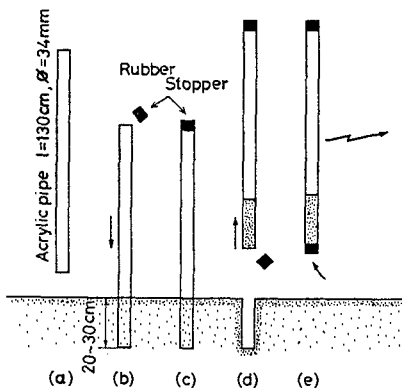


Fig. 1 Method of taking core sample.

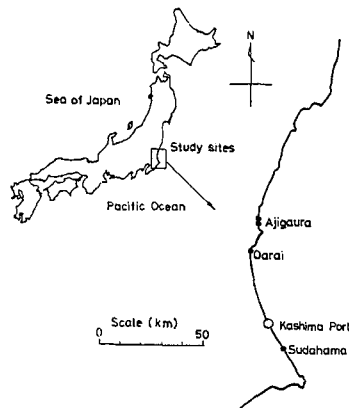


Fig.2 Location of study site.

Table 1 Summary of experiment conditions

Site	Experiment number	H_0 (m)	T_0 (s)	Tide level (m)	Tide level (m)	Clearance (cm)	Sediment d_{50} (mm) S_0, S_k
Oarai	8/31/81	0.52	6.0	0.16	0.77	12, 15	0.24
	9/ 2/81	0.38	5.7	0.36	1.07	8, 8	1.34, 1.12
Sudahama	7/28/82	1.50	8.5	1.03	0.78	12, 20	0.16
	7/29/82	1.20	8.8	0.86	0.90	17, 25	1.17, 0.99
	7/30/82	1.00	8.4	0.75	1.00	20	
Sudahama	8/24/83	1.02	5.7	0.26	1.31		
	8/25/83	0.85	7.5	0.32	1.13	13, 17	

being disturbed. The core sample is then sliced into 2 centimeters segments from the sea bottom to the depth of 12 centimeters. Each segment is well mixed, and about 40 % of its quantity is spread out in the shape of a circular plate having the diameter of 8 centimeters and the thickness of 0.15 centimeter on a flat plate in a pitch-dark room. Then, the number of the sand grains with each tracer color on the surface of the circular plate is counted ocularly under an ultraviolet light.

2.2 Sites of field observations

The tracer experiments were carried out three times on two beaches on the east coast of Japan - Oarai (autumn 1981) and Sudahama (summer 1982, summer 1983). These beaches are classified as micro-tidal beaches, because their tide ranges are about 1 meter. They are exposed to the full wave energy of the Pacific Ocean. The locations of these beaches are shown in Fig.2. An outline of each beach can be found elsewhere (Kato et al., 1985). In total the tracer experiments were carried out for seven days. In this report, each experiment will be referred to by year, month and day.

General conditions of the sea during the field observations are listed in Table 1. The fifth and sixth columns give the tidal levels at the times of start and end of the observations above the datum line. A clearance listed in the seventh column is the vertical distance of the sensor of currentmeter from the sea bottom. The clearance was measured by using a scale or a palm and fingers of a frogman, repeating twice in almost all cases. The last column gives the medium diameter of sand (d_{50}), the sorting coefficient (S_0) and the skewness parameter (S_k) of the beach materials (quartz sand).

The observation was carried out at the ground elevation around the datum level, 0 meter, in each case. This is because of the fact that we could not help deciding the locations of almost the same water depth for the sampling works by the frogmen. The observation points were usually located inside the surf zone in all cases.

3. Characteristics of Waves and Currents

The two horizontal components of current velocities measured at the injection point were digitized at the interval of 0.1 second. Every two consecutive digital data are averaged to yield the smoothed data with the time interval of 0.2 second, which are utilized for analyses.

The representative values of currents, that is to say, the mean velocity, the principal direction of the incident waves (Nagata,1964), the skewness, the root-mean-square value of velocity fluctuation and a velocity atiltness in the principal wave direction, are calculated for every fifteen minutes.

A principal direction of the waves, θ_p , is defined as

$$\tan 2\theta_p = 2\overline{uv}/(\overline{u^2} + \overline{v^2}), \quad (1)$$

where u and v are the horizontal components of wave motions only, which are obtained by removing the steady state currents from the original data.

The velocity component in the principal wave direction U_p , being defined positive in the direction of wave propagation, can be obtained by the coordinate transformation with the angle of θ_p . The skewness is defined for U_p as

$$\sqrt{\beta_1} = \frac{1}{N} \sum (U_p)_i^3 / (U_p)_{rms}^3. \quad (2)$$

The velocity atiltness which is a new parameter originally proposed by Goda (1985) for the forward tilting of wave profile is calculated. The velocity profile of the forward tilting, when it is differentiated with respect to time, yields the up-and-down asymmetry in the acceleration profile, the magnitude of which can be evaluated by the similar way as the skewness as follow:

$$\sqrt{\gamma_1} = \frac{1}{N} \sum (\dot{U}_p)_i^3 / (\dot{U}_p)_{rms}^3, \quad (3)$$

where the overdot in the expression denotes the differentiation with respect to time.

For every observation, the arithmetic means of the representative characteristics of waves and the vectorial means of mean current velocities are calculated for the period from the time of injection to the end of observation, and the resultant values are listed in Table 2.

According to Table 2, the values of skewness in 7/28/82 and 7/30/82 are negative. As the velocity fluctuation due to waves U_p is defined as positive in the direction of wave propagations in these data analyses, the values of the skewness of U_p in the surf zone would be thought positive and large from the analogy of surface wave profiles. Therefore, It is a quite curious fact that the mean values of skewness are negative on Sudahama Beach. Their cause is examined here.

Figures 3 shows typical records of current variations in the case of negative skewness. The direction of the Y-component is almost the same as the direction of the incident wave propagation and that of the X-component is nearly parallel to the shoreline. The current velocity in the Y-component is featured with the existence of long-period fluctuations which have the period of about 80 to 100 seconds and the amplitude much greater than that of the short-period fluctuations corresponding to the motions of incident waves.

Table 2 Representative value of currents and waves

		\bar{v} (cm/s)	$\sqrt{\overline{U_p^2}}$ (cm/s)	velocity skewness	$\sqrt{\overline{U_p^2}}$ (cm/s*s)	velocity atiltness
8/31/81	1	2.27	32.20	0.273	48.95	0.206
	2	2.90	31.20	0.316	47.45	0.177
	3	5.37	30.66	0.354	44.85	0.101
9/ 2/81	1	27.48	28.93	0.719	60.45	0.954
	2	26.23	28.70	0.709	61.20	0.874
	3	22.94	27.92	0.677	63.30	0.725
7/28/82	1	22.88	41.96	-0.266	58.00	0.408
	2	27.15	42.31	-0.289	58.20	0.406
	3	30.14	45.97	-0.131	56.90	0.434
7/29/82	1	49.53	40.97	0.101	44.55	1.040
	2	62.82	43.00	0.195	44.40	1.068
	3	61.17	43.91	0.138	43.80	1.069
7/30/82	1	55.39	53.40	-0.069	43.50	1.075
	2	58.94	53.60	-0.102	44.60	1.002
	3	63.01	52.88	-0.086	45.95	0.951
8/24/83	3	15.97	33.99	0.190	55.30	0.506
8/25/83	3	36.11	45.00	0.049	46.20	0.930

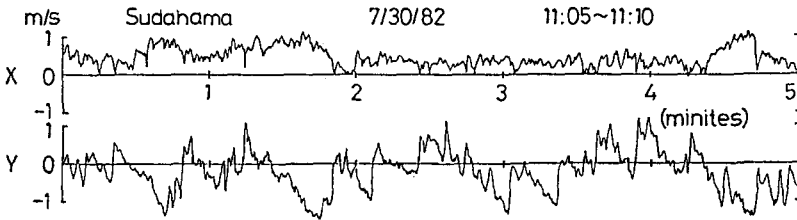


Fig.3 Typical segment of current records

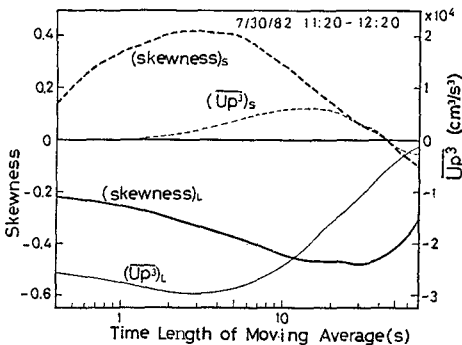


Fig.4 The values of skewness for the long period component and the short one.

By inspecting Fig.3 in detail, we can notice that the long-period components do not fluctuate sinusoidally but in the way that the velocity profile is flattened with longer duration in the positive side (onshore) and is sharpened with shorter duration in the negative side (offshore). Then, two analyses have been attempted for calculating the values of skewness. One analysis is to calculate the value of skewness, which is denoted by $(skewness)_L$, for the smoothed velocity profile which is obtained by the application of the moving average technique; the averaging time length is

varied from 0.45 s to 70 s. Another is to calculate the skewness for the profile with removal of the smoothed profile, which corresponds to that of the relatively short-period components, and the resultant value is denoted by (skewness)_s. These analyses have been done for the time series data of one hour. The result of analyses is shown in Fig.4, where the abscissa denotes the averaging time length. According to this figure, the values of skewness for the long-period components is always negative. Therefore, it is considered that the values of skewness for the long-period fluctuation are negative which make the values of skewness for the velocities combined of short and long-period components to be negative.

4. Characteristics of tracer movements

4.1 Advection speed and its direction

In order to estimate the advection speed and its direction of sand tracer, the following equations which have been derived by Nadaoka et al. (1981) are employed here.

Let $C(\omega, t)$ be the number of tracer particles in a core at the time t after the injection of tracer at a point of the direction ω on the circumference having a radius R (see Fig.5). Up to this time, tracer particles of $C(\omega, t)$ in number are considered to have moved from the center of circle to the circumference. It does not matter how tracer particles were transported there, whether in suspension or not, what happened with them on the way, and which way did they pass through. We are only concerned with the fact that they have moved there with the travelling time of t . Then the components of apparent travelling speed of tracer particles in the directions of η and ξ are given by $(R \cos \omega)/t$ and $(R \sin \omega)/t$, respectively. Furthermore, the mean advection velocity of tracer during the experiment can be defined by the following two components, u_m and v_m :

$$u_m = \frac{\int_0^\infty \int_0^{2\pi} C(\omega, t) \frac{R}{t} \cos \omega d\omega dt}{\int_0^\infty \int_0^{2\pi} C(\omega, t) d\omega dt} \quad (4)$$

$$v_m = \frac{\int_0^\infty \int_0^{2\pi} C(\omega, t) \frac{R}{t} \sin \omega d\omega dt}{\int_0^\infty \int_0^{2\pi} C(\omega, t) d\omega dt} \quad (5)$$

By using Eqs. (4) and (5), we have

$$V_t = (u_m^2 + v_m^2)^{1/2} \quad (6)$$

$$\theta_t = \tan^{-1}(v_m/u_m) \quad (7)$$

where V_t is the mean advection speed of fluorescent sand tracer and θ_t is its direction.

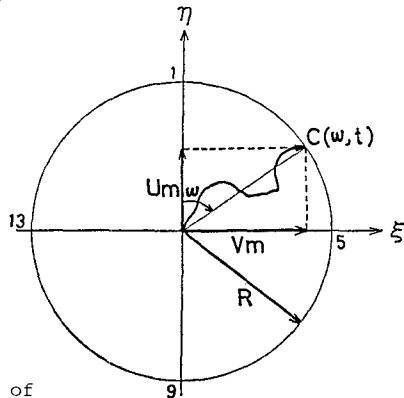


Fig. 5 Coordinate system.

In order to observe clear relations between the tracer advection and the characteristics of waves and currents, an oblique coordinate system which has been introduced by Nadaoka et al. (1981) will be used again. That is to say, the η axis is taken in the principal wave direction and the ξ axis is taken in the mean current direction, as shown in Fig.6. As these two axes generally intersect at an oblique angle, let the angle measured from the η axis to the ξ axis in the clockwise direction be ϕ_s .

Let us assume that the sand advection speed is V_t with the angle ϕ_t , which is defined in the same way as ϕ_s . Furthermore its two components in the directions of the mean current and the wave propagation are denoted by V_s and D , respectively, as shown in Fig.6. Then we have two equations as follows:

$$V_s = V_t \cdot \sin \phi_t / \sin \phi_s \quad (8)$$

$$D = V_t \cdot \cos \phi_t (1 - \tan \phi_t / \tan \phi_s) \quad (9)$$

As all of physical quantities in the right-hand sides in Eqs. (8) and (9) can be estimated by Eqs.(1), (6) and (7) by utilizing the data measured, the values of V_s and D have been calculated and are listed in the first and the second columns in Table 3.

Table 3 Tracer advection speed and mixing depth

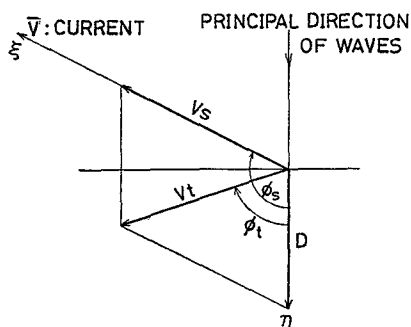


Fig. 6 Oblique coordinate system and definition of symbols.

		V_s (cm/s)	D (cm/s)	Mixing depth (cm)
8/31/81	1	-0.224	-0.063	4.08
	2	-0.100	0.151	3.37
	3	0.019	0.209	3.64
9/ 2/81	1	0.151	0.050	4.09
	2	0.158	0.056	3.96
	3	0.208	0.053	3.60
7/28/82	1	0.516	0.145	4.89
	2	0.183	-0.086	4.89
	3	1.054	0.271	3.77
7/29/82	1	0.188	-1.393	3.59
	2	0.319	-0.806	3.16
	3	0.360	-0.334	3.13
7/30/82	1	0.269	0.070	4.32
	2	0.498	0.150	3.60
	3	0.717	0.281	3.67
8/24/83	3	-0.073	-0.255	4.02
8/25/83	3	-0.182	-0.299	6.53

4.2 Mixing depth of fluorescent sand tracer in the sea bottom

As pointed out by Komar and Inman (1970), Nadaoka et al.(1981) and Kraus (1985), a phenomenon of sand mixing in a layer from the sea bottom surface to some depth exists in the surf zone. The vertical distributions of fluorescent sand tracer are calculated for each tracer with all of the data, and the average mixing depth of 80% cut-off are also calculated and listed in the last column in Table 3. In this report the mixing depth is defined as the depth containing 80% of the

total tracer in a core, in the same manner as Nadaoka et al. (1981) and Kraus (1985).

5. Relations between Local Sand Transport and Fluid Dynamics

5.1 Advection speed of sand movement in the direction of mean currents

Nadaoka et al. (1981) obtained a semi-theoretical relationship of

$$\bar{V}_s = 0.01 * \bar{V}_1. \quad (10)$$

where \bar{V}_s is the mean advection speed of longshore transport and \bar{V}_1 is the average longshore current velocity, and they said with some field data that Eq.(10) is valid for the local sand transport.

The values of the advection speed of tracer in the direction of mean currents V_s and mean current velocity \bar{V} , which are listed in Table 3, are plotted in Fig.7. As seen in Fig.7, the data points, except one point which have relatively larger values of V_s , scatter around a straight line of

$$V_s = 0.01 * \bar{V}. \quad (11)$$

Therefore the relation of Eq.(11) is considered to be reconfirmed here.

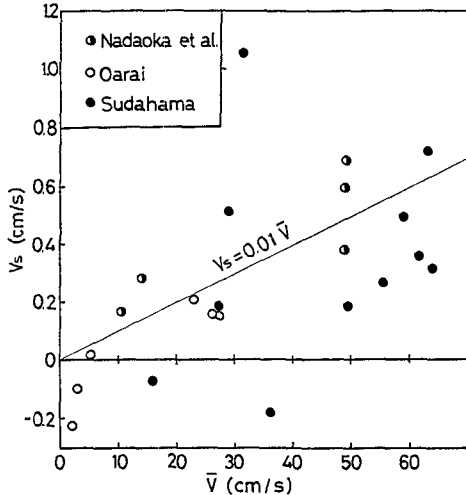


Fig. 7 V_s compared with \bar{V} .

5.2 Advection speed of sand movement in the principal wave direction
 Nadaoka et al. (1981) showed that the dimensionless advection speed in the principal wave direction, $D/\sqrt{U_D^2}$, can be explained by using the skewness parameter, which represents the feature of up-and-down asymmetry of velocity profile. Then, we tried to plot it against the skewness. The dimensionless advection speed, however, can be explained partially but not wholly by using only the skewness parameter (see Katoh et al., 1985), we need to take another parameter into account.

It might be said that the analysis in Nadaoka et al.(1981) has been done for one aspect of sand transport, i.e., bed load transport. Another approach for the explanation of the suspended load transport is thus necessary. Based on the data obtained in the surf zone, Sternberg, Shi, and Dowling (1984) reported that the frequency and duration of individual suspension events were strongly correlated with incident wave conditions, and the events of suspensions were in phase with bores propagating across the surf zone. Therefore, it is better to use a parameter representing the characteristic of the bores which have distinct features of the forward tilting both in the surface profile and in the velocity profile. Then, by using the velocity atiltness parameter (Eq.3), let us assume that the dimensionless advection speed

in the principal direction can be approximately expressed as follow:

$$D/\sqrt{U_p^2} = a \cdot \sqrt{\beta_1} + b \cdot \sqrt{\gamma_1} \cdot (\dot{U}_p)_{\text{rms}}^3 / g^3, \quad (12)$$

where a and b are the coefficients and the second term in the right-hand side is normalized with the third power of the acceleration of gravity.

The transport direction of suspended load should be taken care, because the newly defined parameter is considered to be related to the concentration of the suspended load alone. According to the Shore Protection Manual, Coastal Engineering Research Center (1977), when the ratio of the deepwater wave height to the fall velocity of the beach sediment, H_0/w , is greater than wave period, T, the significant concentration of suspended load are expected to diffuse offshore and deposit in the offshore side. In the cases of the observations reported here, the fall velocity is of about 1.8 cm/s to 3.2 cm/s. If the period of incident waves, about 8 seconds (see Table 1), is taken for T, and 1.0 meter is taken for H_0 , the value of H_0/w is apparently greater than T. Therefore, the suspended load is thought to be transported in the offshore direction.

The above consideration is applicable for the velocity fields due to the incident waves alone, but it is not so for the case in which the predominant long-period components coexist. In the latter case, the direction of the combined velocity depends almost on that of the long-period components. As seen in Fig.3, for example, when the long-period velocity components have a large positive value, the velocity combined with those of incident waves fluctuate mainly in the positive side. Under these conditions, a practice of taking the period of the incident waves as T is not appropriate, because the suspended load due to the passing of bores will be transported in the direction of the velocity of long-period components.

The direction of the net suspended load transport in the velocity fields containing the predominant long-period components will be inferred as follows. The values of skewness for the long-period velocity components are negative, which means that the total duration of the time when the direction of velocity is onshore is longer than that of offshore. The high concentration of suspended load occurs when the bores pass through. If the time interval between two arriving bores is constant, the frequency of the bores passing through a fixed point becomes larger during the time periods of onshore velocities than those of offshore ones, because the duration of the former is longer than that of the latter. This situation can be recognized in Fig.3. Therefore, the larger amount of sand is transported to the onshore direction in suspension, which yields the net onshore transport.

The sign of the coefficient b should be changed based on whether the predominant long-period components coexist or not with the incident waves. For this purpose, the values of skewness or U_p^3 can be utilized as a first step, because it is positive when the incident wave components are relatively large and is negative when the long-period components are relatively large. Thus, Eq.(12) is rewritten as

$$D/\sqrt{\bar{U}_p^2} = a \cdot \sqrt{\beta_1} + b \cdot \text{sgn}(\sqrt{\beta_1}) \cdot \sqrt{\gamma_1} \cdot (\dot{U}_p)_{\text{rms}}^3 / g^3, \tag{13}$$

where $\text{sgn}(\sqrt{\beta_1})$ takes the value of +1 or -1 depending on whether the skewness is positive or negative, and the value of redefined coefficient b should be a negative.

The value of \bar{U}_p^3 can be obtained by multiplying the third power of $\sqrt{\bar{U}_p^2}$ by the skewness of the acceleration profile which are listed in Table 2. Using a regression analysis for Eq.(13) with the data listed in Table 2, we get the values of 0.024 and -85.1 for a and b, respectively. In turn, the value of the quantity in the right-hand side of Eq.(13) for each sand tracer has been calculated with the values of coefficients obtained, and it is plotted on the abscissa with the corresponding dimensionless advection speed on the ordinate in Fig.8.

Except three data points, the data are gathered around a straight line having the inclination of 0.85. The straight line is decided by applying the least squares method to the data excluding the three distant points so that the line should pass through the origin. By multiplying the coefficients a and b with the value of 0.85 we have the following relation:

$$D/\sqrt{\bar{U}_p^2} = 0.02\sqrt{\beta_1} - 72.4 \cdot \text{sgn}(\sqrt{\beta_1}) \cdot \bar{U}_p^3 / g^3 \tag{14}$$

The first term in the right-hand side of Eq.(14) is considered to correspond to the bed load transport, while the second one to the suspended load transport. Equation (14) indicates that the directions of bed and suspended load transports are opposite each other, because \bar{U}_p^3 usually takes a positive value.

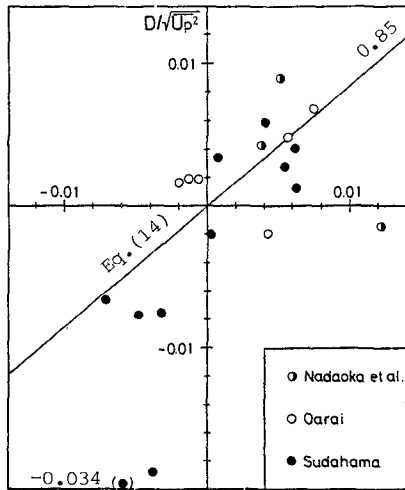


Fig.8 $D/\sqrt{\bar{U}_p^2}$ compared with the skewness and magnitude of forward inclination of velocity profile.

5.3 Mixing depth of sand tracer

Sunamura and Kraus (1985) presented the shear stress model to predict the average depth of wave-induced sediment mixing in the surf zone. The model shows that the mixing depth normalized with the sediment grain diameter is linearly related to the Shields parameter, which is proportional to the square of the velocity of the breaking waves. Then, let us examine whether this relation can be applied to the local mixing depth and the local velocities or not. The mixing depths listed in Table 3 are plotted against the mean-square values of velocities divided by the gravity of acceleration, U_p^2/g , in Fig.9. Although some scatter is observed in the data points, the straight line drawn through the origin gives the result of

$$\bar{b} = 2.5 * U_p^2 / g. \tag{15}$$

Equation (15) can be rewritten with the local wave height by using the some assumptions as

$$b = 0.10 * H_{1/3}. \tag{16}$$

This result is nearly same as that of Nadaoka et al. (1981) for the data obtained at Ajigaura Beach, in which the value of coefficient is about 0.08.

Furthermore, by assuming a constant sloping beach, $h = x \tan\beta$, and $\gamma = H_{1/3}/h = 0.6-0.65$ in the case of irregular waves in the surf zone, the average mixing depth in the surf zone can be estimated as follow:

$$\bar{b} = \frac{1}{X_b} \int_0^{X_b} b dx = \frac{1}{X_b} \int_0^{X_b} 0.10 \cdot \gamma \cdot x \tan\beta \cdot dx = 0.05 \cdot H_b, \tag{17}$$

where X_b is the width of the surf zone and H_b is the significant wave height at the wave breaking point. The value of coefficient in Eq.(17) is of the same order as that in Sunamura and Kraus (1985), that is to say 0.027, but the former is about twice as large as the latter. At least in this report, the mixing depth should be expressed in terms of the velocity fluctuations as in Eq.(15), because the local wave height have not been measured in our observations.

5.4 Local sand transport rate

In much the same way as the bulk volume of longshore sand transport rate (Komar and Inman, 1970), a bulk volume of local sand transport rate per unit width Q_t is given by the equation

$$Q_t = b * V_t. \tag{18}$$

The local advection velocity of the sediment V_t has been decomposed into the two components V_s and D in the directions of mean currents and the incident waves, respectively. The local sand transport rate is also decomposed into such two directions as follows:

$$Q_s = b * V_s, \tag{19}$$

$$Q_D = b * D. \tag{20}$$

By substituting Eqs.(11), (14) and (15) into Eqs.(19) and (20) respectively, we have

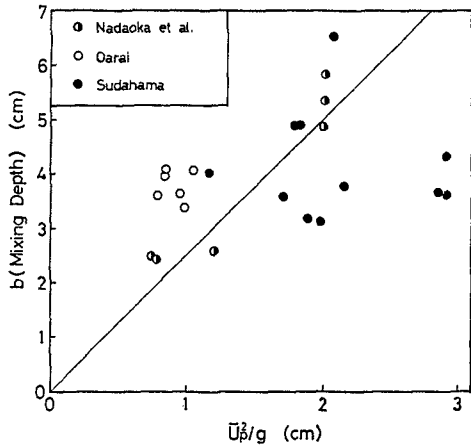


Fig. 9 Local mixing depth compared with U_p^2/g .

$$Q_s = \frac{0.0025}{g} * \overline{U_p^2} * \overline{V}, \quad (21)$$

$$Q_D = \frac{1}{g} [0.05 \cdot \overline{U_p^3} - 181 \cdot \text{sgn}(\overline{U_p^3}) \cdot (\overline{U_p^2})^{3/2} \cdot \overline{U_p^3} / g^3] \quad (22)$$

The first term in the right-hand side of Eq.(22) mainly corresponds to the bed load transport, while the second one to the suspended load transport. Based on Eq.(22), further interesting discussions can be made. The mixing depth b is multiplied by the second term in the right-hand side of Eq.(14) to yield the contribution of suspended load to the total sand transport rate in Eq.(22). This operation looks strange because the mixing process is a phenomenon in the sea bottom, whereas the suspension of the bed material is that above the sea bottom. This apparent strangeness, however, may serve to understand the mechanics of sand transport in suspension in the surf zone.

For simplicity, let us pay our attention to one sand particle which has the same diameter as the others. The particle pausing on the sea bottom surface at first is suspended when the bore passes over it. Subsequently it is transported in suspension to some distance with the same velocity as the fluid one and deposit after several seconds on the sea bottom. Next, it is buried into the sea bottom due to the some mixing process of bed material. Then it loses an opportunity to be suspended again for a while. The time required for the particle to emerge again on the sea bottom surface becomes longer with increase in the mixing depth of the bed material. The elongation of the reappearance time reduces the apparent advection speed. This effect is already contained in the empirically obtained advection speed D (the second term of the right-hand side of Eq.14). While it is being buried in the sea bottom, the other particles which have been buried in the sea bottom to some depth initially at that point are successively suspended and transported to other points, of course with the same apparent advection speed as that of the particle we pay our attention to. The number of these particles suspended, or bulk volume of the particles, becomes large with increase in the reappearing time of our particle which is inferred to depend on the mixing depth b . Therefore, in order to obtain the total bulk volume of sand transport rate in suspension, the mixing depth b should be multiplied by the advection speed such as the second term in the right-hand side of Eq.(22).

Discussions have actively been held concerning whether the suspended load or the bed load transport is more important in the surf zone. For examples, Komar (1978) concluded that the suspended load is much less significant than the bed load transport, while Sternberg, Shi and Downing (1984) reported that all of the longshore transport at Leadbetter Beach could be accounted for by the suspended load transport. Let q_b and q_s be the absolute values of bed load and suspended load transport rate in the principal wave direction, respectively. They can be expressed from Eq.(23) as follows:

$$q_b = |0.05 \cdot \overline{U_p^3}| / g, \quad (23)$$

$$q_s = |181 \cdot (\overline{U_p^2})^{3/2} \cdot \overline{U_p^3}| / g^4, \quad (24)$$

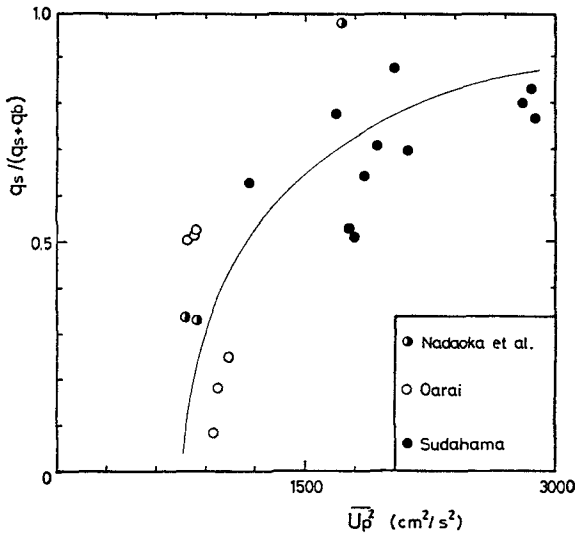


Fig. 10 Rate of suspended load transport compared with $\overline{U_p^2}$.

where $\text{sgn}(\overline{U_p^3})$ is neglected because it has the absolute value of unity. Utilizing the values listed in Table 2, we can calculate the values of $q_s / (q_s + q_b)$ on the basis of Eqs.(23) and (24). The obtained values are plotted on the ordinate against the values of $\overline{U_p^2}$ on the abscissa in Fig.10. According to Fig.10, the ratio of the absolute suspended load transport to the total transport varies among the values of less than 0.1 to nearly 1.0 with a tendency of increase with the mean-square value of the velocity in the principal wave direction. From this tendency of increase, it can be inferred that the suspended load transport will become more significant under the high wave conditions.

6. Summary

The major conclusions in this report are as follows:

- (1) It is reconfirmed that the advection speed of sand tracer in the mean current direction is about 1 % of the mean current velocity.
- (2) The advection speed of sand tracer in the principal wave direction depends on not only the up-and-down asymmetry but also the before-and-behind asymmetry in the velocity profiles. The former asymmetry is considered to be related to the bed-load transport and the latter one to the suspended load transport. The magnitude of the before-and-behind asymmetry is evaluated by calculating the skewness for the acceleration profiles.
- (3) The local mixing depth of the bed material is approximately proportional to the mean-square value of fluid velocities, which suggests the linear relationship with the local wave height.

(4) For the first approximation, the equations for the local sand transport rate are proposed which are restricted to the field conditions under which the observations have been carried out.

(5) The transporting conditions of suspended load are inferred so that the bed material may be intermittently transported in suspension in relatively short durations and be buried in the sea bottom due to the process of mixing of bed material during the remaining periods.

(6) The suspended load transport will become more significant under the high wave conditions.

The local sand transport rate equations empirically obtained in this study are not necessarily enough, because the local bottom slope, sediment characteristics, the critical velocity of the onset of sand movement and other factors are not taken into account and the assumption in the form of Eq.(13) is for the first approximation. Furthermore, it is a question whether the fluid velocities at the point of about 20 cm above the sea bottom is appropriate or not to be related with the sand transport rate. It is, however, clear for the local sand transport in the onshore-offshore direction that both the up-and-down and the before-and-behind asymmetry in the velocity profiles are important factors.

Acknowledgements

The authors should like to express their heartfelt thanks to Dr.Kazuo Nadaoka, Tokyo Institute of Technology, for his contributions on the field observations when he was a member of the Littoral Drift Laboratory, the Port and Harbour Research Institute.

References

- Coastal Engineering Research Center, U.S.Army (1977): Shore protection manual, U.S.Government Printing Office, Vol.1, pp.4-81 to 4-84.
- Goda, Y. (1985): Numerical examination of several statistical parameters of sea waves, Report of the Port and Harbour Research Institute, Ministry of Transport, Japan, Vol.24, No.4 (in Japanese).
- Katoh, K., N. Tanaka, T. Kondoh, M. Akaishi and K. Terasaki (1985): Field observation of local sand movements in the surf zone using fluorescent sand tracer, Report of Port and Harbour Research Institute, Vol.24, No.4, pp.3-63.
- Komar, P.D. and D.L.Inman (1970): Longshore sand transport on beaches, J.G.R., Vol.75, No.30, pp.5914-5927.
- Komar, P.D. (1978): Relative quantities of suspension versus bed-load transport on beaches, J. of Sedimentary Petrology, Vol.48, pp.921-932.
- Kraus, N.C. (1985): Field observations on vertical mixing of sand in the surf zone, Jour. of Sedimentary Petrology, Vol.55, No.1, pp.3-14.
- Nadaoka, K., N. Tanaka and K. Katoh (1981): Field observation of local sand movements in the surf zone using fluorescent sand tracer, Port and Harbour Research Institute, Vol.20, No.2, pp.75-126 (in Japanese).
- Nagata, Y. (1964): The statistical properties of orbital wave motions and their applications for the measurement of directional wave

spectra, *Jour. of Oceanographical Soc. of Japan*, Vol.19, No.4, pp.169-181.

Sternberg, R.W., N.C. Shi and J.P. Dowing (1984): Field investigations of suspended transport in the nearshore zone, *Proc. 19th Int. Conf. on Coastal Eng.*, pp.1782-1798.

Sunamura, T. and N.C. Kraus (1985): Prediction of average mixing depth of sediment in the surf zone, *Marine Geology*, 62, pp.1-12.